

## Surface and Subsurface Flow System Configuration for Conjunctive use Management at Regional Scale

Sina NASOUHI\*, Toshio HAMAGUCHI and Toshiharu KOJIRI

\*Graduate School of Engineering, Kyoto University

### Synopsis

The application of conventional conjunctive use models has been mainly restricted to plain fields, and under limited recharge scenarios. The current research, however, tries to propose a modeling frame work that can address these two problems. In the previous report, a series of analytical solutions for generating primary operation rules was provided. As the second step, this report expands the modeling domain from plain area up to the mountainous sub-basins, by developing a DEM-based channel configuration algorithm for a sub-basin of the Nagara River. The algorithm unlike common GIS software can handle the error resulted from up lifting topographical sinks, and was proved to be practical for hydraulic routing on variable topography.

**Keywords:** conjunctive use, flow direction, iso-parametric approximation

## 1. Introduction

### 1.1. Research overview

The application of conventional conjunctive use models has been restricted mainly to plain area under limited hydrological scenarios. To generate the required long-term inflow for driving operation rules, the authors developed a series of analytical solutions for simultaneous recharge estimation. Then based on the delay in surface and ground water inflow (Fig.1) and mass curve analysis (Fig.2), a simple conjunctive use operation rule

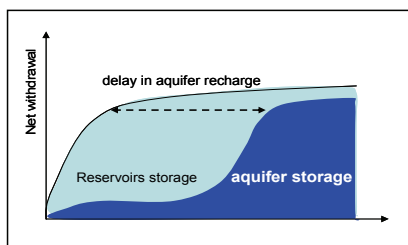


Fig. 1 effect of inflow delay on allocation of surface and ground water resources

was proposed, which could impose upper and lower limits on the net system withdrawal (see Nasouhi *et al.*, 2006). Thus, the limitation of hydrogeological scenarios was relaxed. This net permissible withdrawal later has to be re-distributed through the

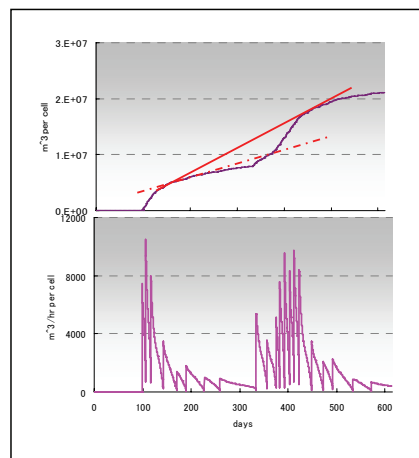


Fig. 2 the long term mass curve analysis (solid tangent) of recharge provides better estimation of the net permissible withdrawal, compared with the short term one (dashed).

model cells (*i.e.* pumping wells and dams) with restricts on environmental vulnerability such as soil salinity. As the second feature of our conjunctive use model, this report considers extending the modeling domain up to the marginal mountainous sub basins, where the impacts of environmental changes such as snow melting on the operation rules can be considered.

## 1.2. Problem identification

A suitable model for conjunctive use applications needs not only to be simple enough for generating operation rules; but also to be able to simulate the dominant hydrological processes in each sub domain (Table.1). This heterogeneity in hydrogeologic settings suggests simplification of the governing equations.

An example is when a simple hydraulic routing over such a variable topography is desired. Traditionally, 1D kinematic wave model in the eight flow directions has met the required simplicity for mountainous basins. However, Liu *et al* (2004) could show that the concentration flow lines of overland flow mainly depend on the hill slope landform, rather than average geometric characteristics as it's applied in 1D kinematic wave model. As an approach, they applied the iso-parametric theory to approximate 2D flow direction over quadrilateral topographical elements. Next, based on a 2D kinematic wave model (Tayfour and Kavas, 1994, and Tayfur, 2001), they introduced a FVM kinematic wave model.

Obviously, kinematic wave theory has to assume a minimum slope in an arbitrary direction under supercritical condition. This assumption however for the DEM-based topography might not be correct,

since the cells with very low or zero gradients can be expected in DEM data.

That is especially important since DEM-based techniques have attracted many interests, due to their capability for utilizing GIS data and RIS analysis. Alternatively, diffusion wave models have been used to handle very low slopes, though they usually need linearization and are not as simple as kinematic wave. As an alternative, Jain *et al* (2005) applied a 2<sup>nd</sup> order FVM diffusion wave model which was easier and more efficient than common 2<sup>nd</sup> order FDM kinematic wave models.

Yet, because of discrete nature of DEM data, unreal sinks in the drainage pattern can be obtained. These sinks, that here after we call "DEM sinks", can result in discontinuity in the drainage network. The software like Arc GIS usually uplift such DEM sinks to connect different channel reaches into a wide network. However, this uplifting mechanism may reduce the average basin elevation and slope, and underestimate runoff velocity consequently. Further, connecting all reaches into a network may not be realistic for arid regions where the drainage network is not developed well, and can be discontinuous.

## 1.3. Report objectives

Despite the variety of our research objectives, this report mainly focuses on surface and subsurface flow configuration at regional scale of conjunctive use. Thus after a brief proposal for subsurface flow, the main body of report deals with developing an effective DEM-based algorithm for surface flow parameterization with application for a sub-basin of the Nagara River Basin.

Table 1 different hydro-geologic setting and process in conjunctive use domain

	<b>mountainous river basin area</b>	<b>flatter area and plains</b>
<b>hydro-geologic setting</b>	- shallow local subsurface storages - rivers are mainly "gaining" type	- deep large aquifers - rivers are mainly "loosing" type
<b>dominant hydrologic process</b>	- saturation excess overland flow - lateral subsurface flow to river (through flow, interflow, base flow)	- infiltration excess overland flow - vertical percolation to the aquifers
<b>hydraulic routing</b>	- kinematic wave model - Conceptual-layers modeling	- diffusion wave - profile modeling (1D Richard equation)

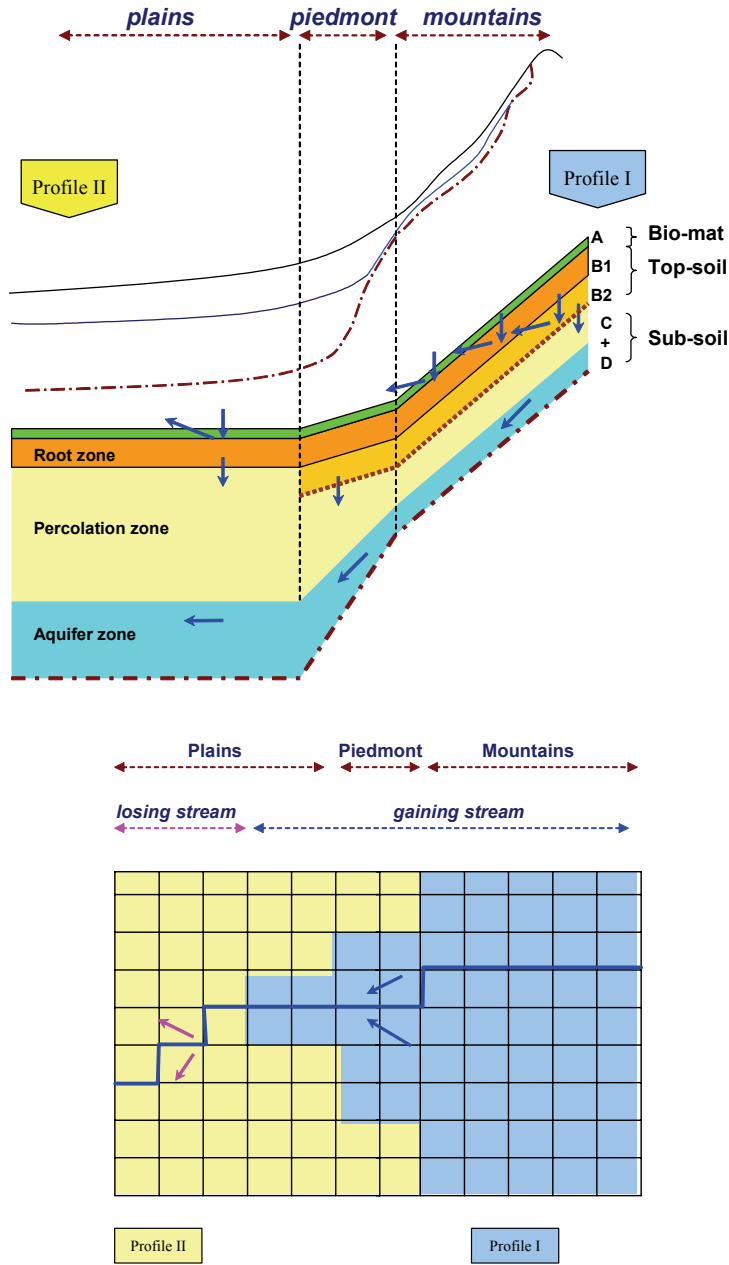


Fig. 3 Proposed modeling layout for subsurface flow configuration, in cross sectional view (above) and plan view (down)

## 2. Subsurface flow configuration

Solution of Richard Equation for the complex hill slope system is not always accurate. That is especially true in mountainous area where geologic discontinuity (*e.g.* faults), and permeable bed rock (*e.g.* fractured rocks) can be quite prevalent. In such condition, defining a continuous domain, and imposing lower boundary conditions at large mesh size can be a challenge. As a simplification, distributed conceptual layered models have been

developed. These models basically involve continuity equation and a steady state form of momentum equation (*i.e.* Darcy law) into a linear or non-linear storage framework. This research developed a transient reformulation under non-linear storage assumption, and linked that to the generalized piston flow equations for the flat downstream areas (Nasouhi *et al*, 2006). The schematic flow components are illustrated in Fig.3.

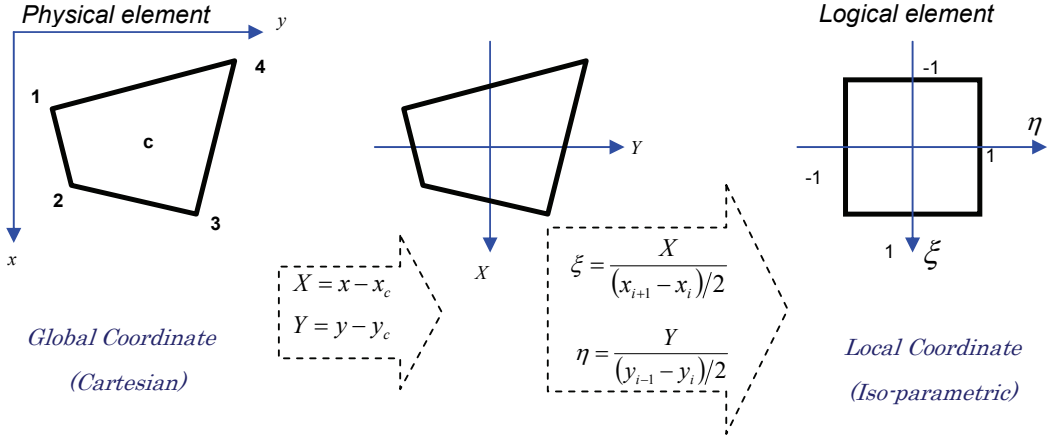


Fig. 4 Iso-parametric transformation of Cartesian coordinate system

### 3. Overview of iso-parametric approximation for flow direction

Liu *et al* (2004) adopted iso-parametric techniques from the finite element method (FEM), to estimate slope for a bi-linear cell in the finite volume method (FVM). A linear interpolation function ( $N_i$ ) thus can be used to estimate dependent variable over a bi-linear cell, in terms of its nodal values as below:

$$N_i(x, y) = \psi(x)\phi(y) \quad (1)$$

Where the linear functions are:

$$\psi(x) = \frac{(x - x_{i+1})}{(x_{i+1} - x_i)}, \quad \phi(y) = \frac{(y - y_{i-1})}{(y_{i-1} - y_i)}$$

The interpolation functions then after iso-parametric transformation of the element (Fi.4) can be expressed as the local shape functions:

$$\eta = \frac{Y}{(y_{i-1} - y_i)/2}, \quad \xi = \frac{X}{(x_{i+1} - x_i)/2} \quad (2)$$

To obtain a general equation, the resulting shape function has been calculated for each node of the quadrilateral element ( $i=4$ ) as follows:

$$i = 1 \therefore \xi = -1 \quad \eta = -1$$

$$\Rightarrow \tilde{N}_1(\xi, \eta) = \frac{1}{4}(1 - \xi)(1 - \eta)$$

$$i = 2 \therefore \xi = 1 \quad \eta = -1$$

$$\Rightarrow \tilde{N}_2(\xi, \eta) = \frac{1}{4}(1 + \xi)(1 - \eta)$$

$$\vdots \quad i = I \therefore \xi = \xi_I \quad \eta = \eta_I$$

$$\Rightarrow \tilde{N}_i(\xi, \eta) = \frac{1}{4}(1 + \xi_I \xi)(1 + \eta_I \eta) \quad (3)$$

Considering the equation (3), now the partial derivative over each element can be estimated:

$$\begin{aligned} \frac{\partial \tilde{f}}{\partial \xi} &= \frac{1}{4} \sum_{i=1}^4 \xi_i (1 + \eta_i \eta) \cdot f_i = \frac{1}{4} \left\{ -f_1(1 - \eta) \right. \\ &\quad \left. + f_2(1 - \eta) + f_3(1 + \eta) - f_4(1 + \eta) \right\} \end{aligned} \quad (4)$$

$$\begin{aligned} \frac{\partial \tilde{f}}{\partial \eta} &= \frac{1}{4} \sum_{i=1}^4 \eta_i (1 + \xi_i \xi) \cdot f_i = \frac{1}{4} \left\{ -f_1(1 - \xi) \right. \\ &\quad \left. - f_2(1 - \xi) + f_3(1 + \xi) + f_4(1 + \xi) \right\} \end{aligned} \quad (5)$$

Finally, by substituting the transformation equations into the chain rules, the partial derivatives in global (Cartesian) system can be estimated:

$$\frac{\partial f}{\partial x} = \frac{\partial \tilde{f}}{\partial \xi} \cdot \frac{\partial \xi}{\partial x} = \frac{\partial \tilde{f}}{\partial \xi} \cdot \frac{2}{dx}$$

$$\Rightarrow \frac{\partial f}{\partial x} = \frac{1}{2dx} (-f_1 + f_2 + f_3 - f_4) \quad (6)$$

#### 4. DEM-based channel network configuration

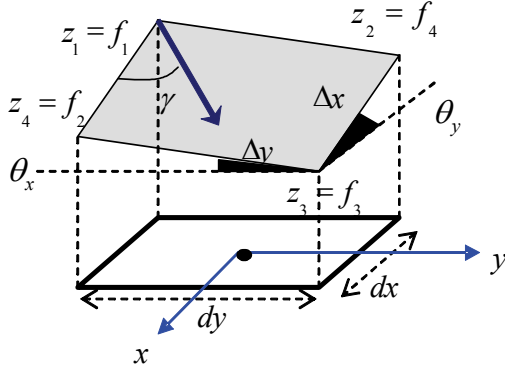


Fig. 5 Adaptation of subscripts from FEM to DEM data

$$\frac{\partial f}{\partial y} = \frac{\partial \tilde{f}}{\partial \eta} \cdot \frac{\partial \eta}{\partial y} = \frac{\partial \tilde{f}}{\partial \eta} \cdot \frac{2}{dy}$$

$$\Rightarrow \frac{\partial f}{\partial y} = \frac{1}{2dy} (-f_1 - f_2 + f_3 + f_4) \quad (7)$$

It's quite feasible to partition hill slope surface in to rectangular finite difference grid with calculation node at the center of projection of each cell (Fig.5). One can replace the nodal values (counterclockwise) with DEM data (clockwise) to reach the similar formulas by Liu *et al* (2004). Yet, the negative unit coefficient here we obtained (equations 10 and 11) indicates negative slope gradient in flow direction. That is physically more sensible than considering positive values for slope vectors when they are in the x or y directions – as it can be concluded from their equations.

$$\tan \theta = |\nabla Z(x, y)| = \sqrt{\left(\frac{\partial z}{\partial x}\right)^2 + \left(\frac{\partial z}{\partial y}\right)^2} \quad (8)$$

$$\tan \gamma = \frac{\partial z}{\partial y} / \frac{\partial z}{\partial y} \quad (9)$$

where

$$\frac{\partial z}{\partial x} = -\frac{1}{2dx} (z_1 + z_2 - z_3 - z_4) \quad (10)$$

$$\frac{\partial z}{\partial y} = -\frac{1}{2dy} (z_1 - z_2 - z_3 + z_4) \quad (11)$$

Liu *et al* (2004) suggested their method for two kind of topographies, including the simple slopes with small grooves (small scale), and the complex slopes with large landform undulation (large scale). However, their application was limited at small scale for the analysis of runoff erosion mechanism, (rill erosion). They let inflow from all nearby cells without any restriction of channel boundaries. Obviously, at large mesh size, the channel reaches have to be located between converging slopes to prevent up-hill flow at such large distances. However, dealing with DEM-based data, one can come across with DEM sinks in the resulting channel network. At this chapter, we try to develop a standard technique to get over these problems.

#### 4.1. Basin topography modeling

Despite of varieties of topography modeling techniques, what we mean by topography modeling here, is such modeling which can accommodate a more compatible channel network to the real drainage pattern. This definition enables us to mark DEM data anomalies; and to approximate them with average values, in such manner that the false sinks disappear and the missing channels can be recovered.

In practice the number of such anomalies can be too large to be adjusted. For instance, a primitive investigation of DEM data in a small sub basin of the Nagara River revealed 100 sinks with the average relative depth of 137.2 m. Consequently the calculated channel network included several discontinuities and reverse slopes.

A simple automatic filter can be defined as the 4-points average of the adjacent DEM data. As the new sinks can be introduced after filtering initial sinks, this filtering procedure should be done in an iterative manner. Thus for our case study, the total initial and secondary sinks came up to 260 points. Note that the default 4-point average filter can be reduced to 3- or 2-points schemes through later manual controls. Yet, for our sub basin, from the 260 points, only 7 sinks had to be re-calculated by 2-point averaging schemes. That indicates the efficiency of 4-point averaging filter.

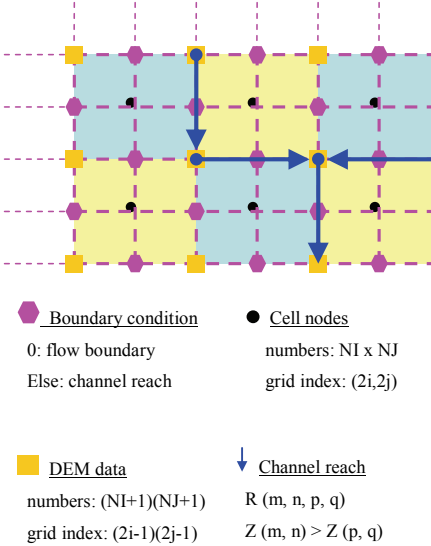


Fig. 6 Control grid worksheet elements

#### 4.2 Channel reaches connection

While discontinuity in simulated channel network can be expected at some special settings (*e.g.* arid regions or karstic terrains); it can be also an error due to missing-data at large DEM mesh size. Obviously, a search radius can be decided where the explicit channel reaches (*i.e.* at the converging slopes) can be connected through possible DEM paths.

To facilitate this, a control grid worksheet was defined where the reaches are demonstrated as vectors at cell boundaries (Fig.6). Note that for each assumed radius, the search has to be repeated to capture secondary connectors in the second step. The procedure has been demonstrated in Fig.7 where the boundary values of 1 and 2 absolute magnitude shows the initial and secondary connectors within unit search radius. Similarly, the absolute values of 3 and 4 stand for twice unit

search radius, respectively. Thus, the developed control grid worksheet provides an efficient interface for later manual control, where the unrealistic connectors can be turned off, by setting zero at boundaries; or the missed connectors can be recovered by defining non-zero values(6 or -6 in this study) for cell boundary condition (Fig.8).

#### 5. Results and discussion

Although conventional DEM sinks filtering can save model from reverse slopes and failure in routing procedure; it can also introduce unrealistic raise in the average basin elevation. It can be seen in Fig.9, where uplifting of DEM sinks with the same surrounding ridges elevation results in moderate hill slopes. Consequently, the discharge rate of lateral inflow to channels can be underestimated. One simple way of correcting this error can be subtracting an averaged estimation of the up-lift, from all those DEM data which lie along the channel system. Hence, while the essential channel slope for establishing continuous flow has been preserved, the nearby slopes have been increased in such a way that the average basin elevation stays the same level. As for the sub basin, the average DEM sinks up-lift was estimated about 137.2 m through 263 sinks. Considering total 322 DEM data on channel network, it suggests an average subtract of -112.06m for each of the channel DEM points. Hence, not only the resulting average basin elevation will be the same as the original data (Fig.9), but also it guarantees a more realistic channel network for the later routing procedure.

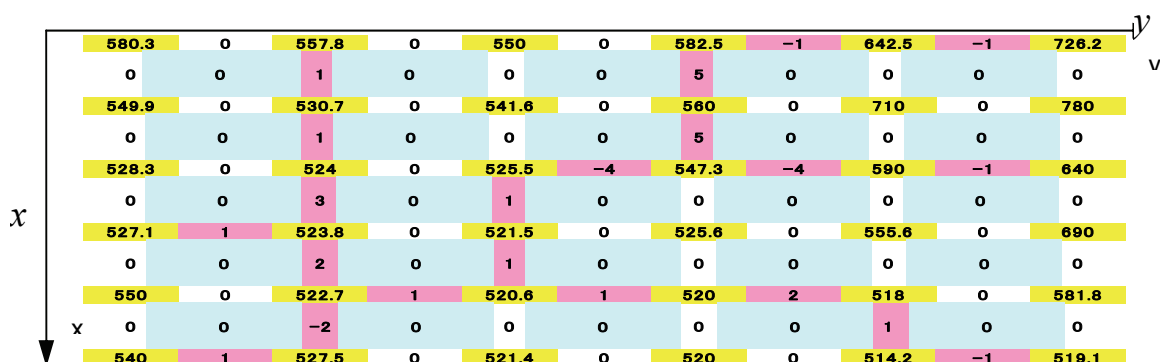


Fig. 7 Demonstration of explicit channels (type 1), and connector channels within 1 unit mesh size (types 2 and 3), and within 2 unit mesh size (types 4 and 5).

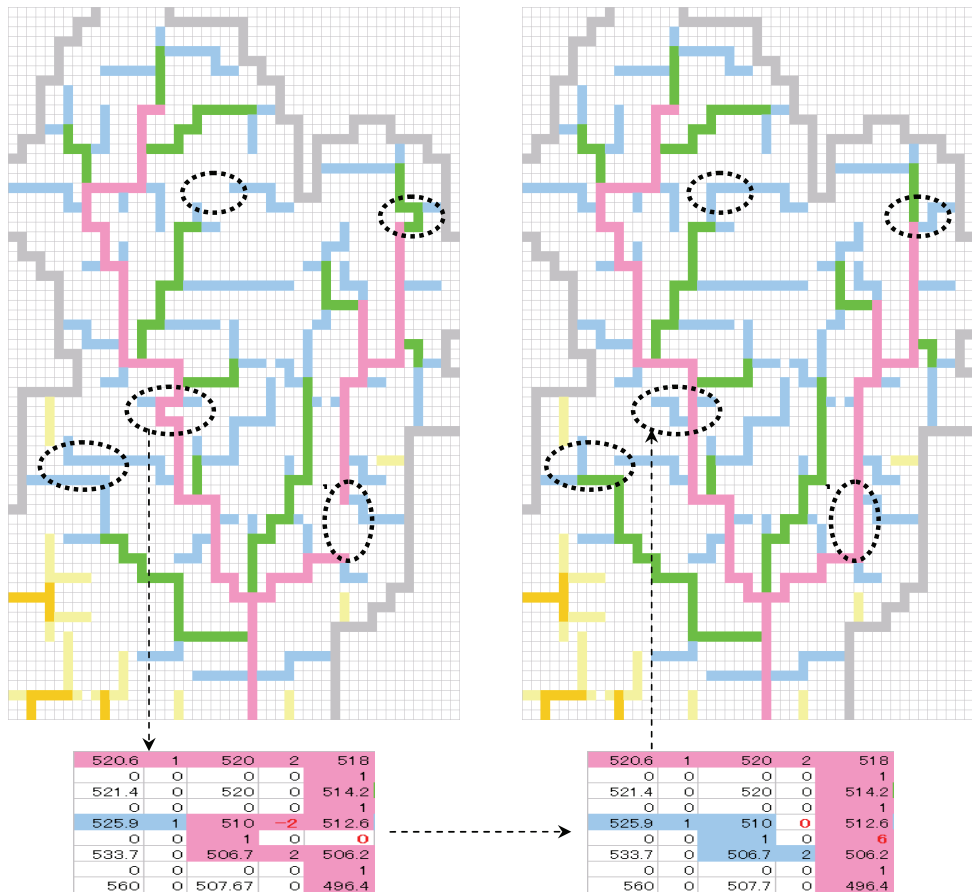


Fig. 8 Channel network improvement (right) after manual control of calculated connectors (left) by changing boundary condition, such as the red values (the lower matrixes). Note that the explicit channels (1 or -1) can not be changed. Also, the manually introduced connectors (6 or -6) need to follow DEM matrix. The gray cells depict sub basin boundaries (the Nagara River Basin)

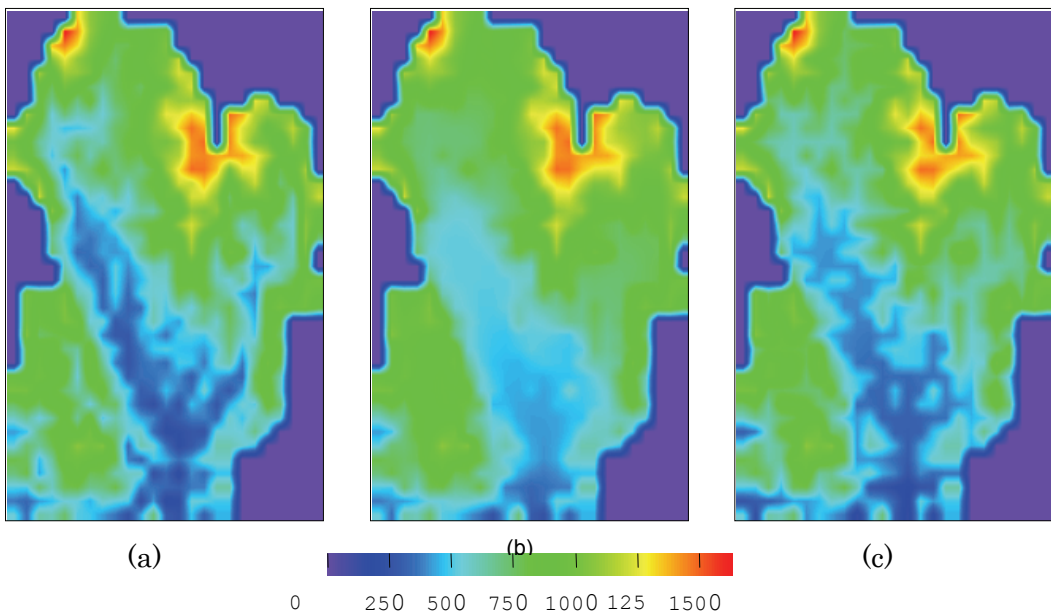


Fig. 9 Topography based on large size mesh DEM data including sinks (a), after filtering the sinks (b), and after un-doing the filtering error (c). The colored scale represents the elevation above sea level (m).

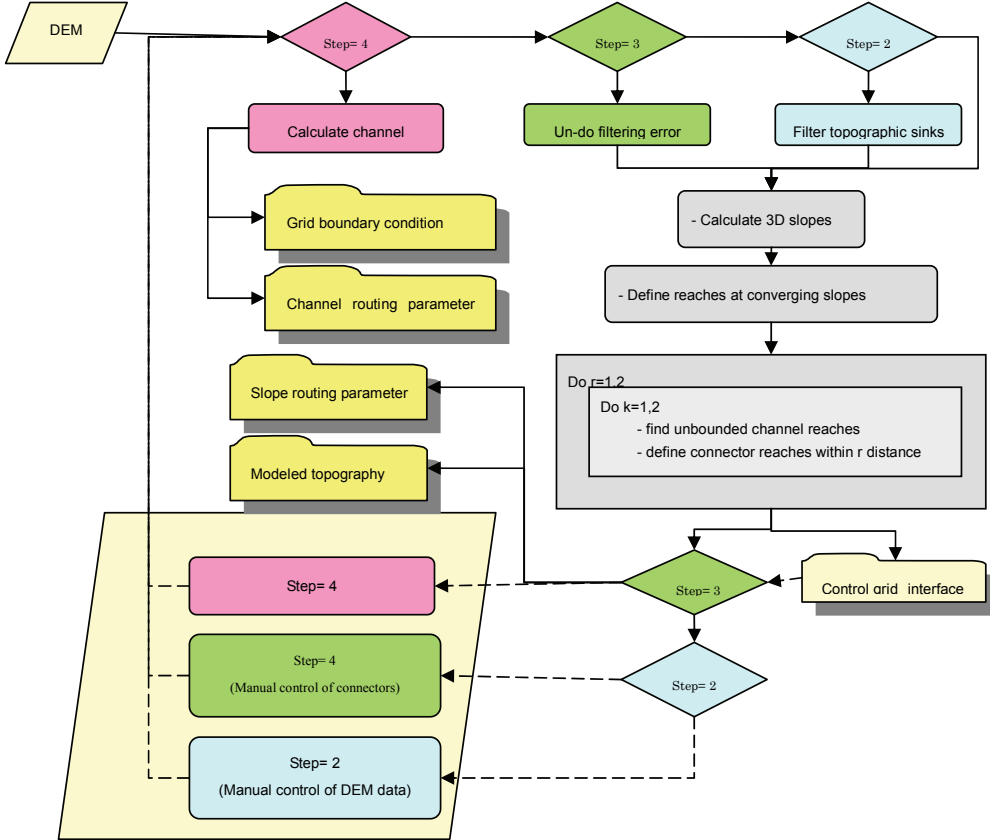


Fig. 10 Final Channel network configuration algorithm with parameterization for surface flow routing

As a byproduct of such pushing down the channel network, the slope of adjacent cells to the network increase in such a way that many of the former connectors (implicit channels) now are locating between the new converging slopes, as the new explicit channels (table 2). This is another merit of our proposed error redistribution technique. Though, as can be seen in Fig.10, the resulting network need to be controlled as usual.

It is essential to mention that our estimation for the average subtract based on changes in channel DEM data is quite basic, and can be replaced by

more accurate estimators such as Equation (12) which apply difference between real average basin elevation and the average elevation of the model after filtering the DEM sinks. Though, the suggested correction algorithm still remains practical enough:

$$\Delta \bar{h} = \frac{\bar{h}_{\text{basin}} - \bar{h}_{\text{model}}}{N_{\text{DEMC}}} \quad (12)$$

where  $N_{\text{DEMC}}$  is the number of the DEM points on the channel reaches.

Table 2 Changes in number of explicit and implicit channel reaches

	after filtering sinks	after DEM adjustment	After undoing the error
<b>Explicit channels</b> (type 1)	229	230	310
<b>Connector channel</b> (type 2)	53	57	27
<b>Connector channel</b> (type 3)	6	5	1
<b>Connector channel</b> (type 4)	24	20	4
<b>Connector channel</b> (type 5)	2	2	0
<b>Manual changes</b> (type 6)	-	10	2

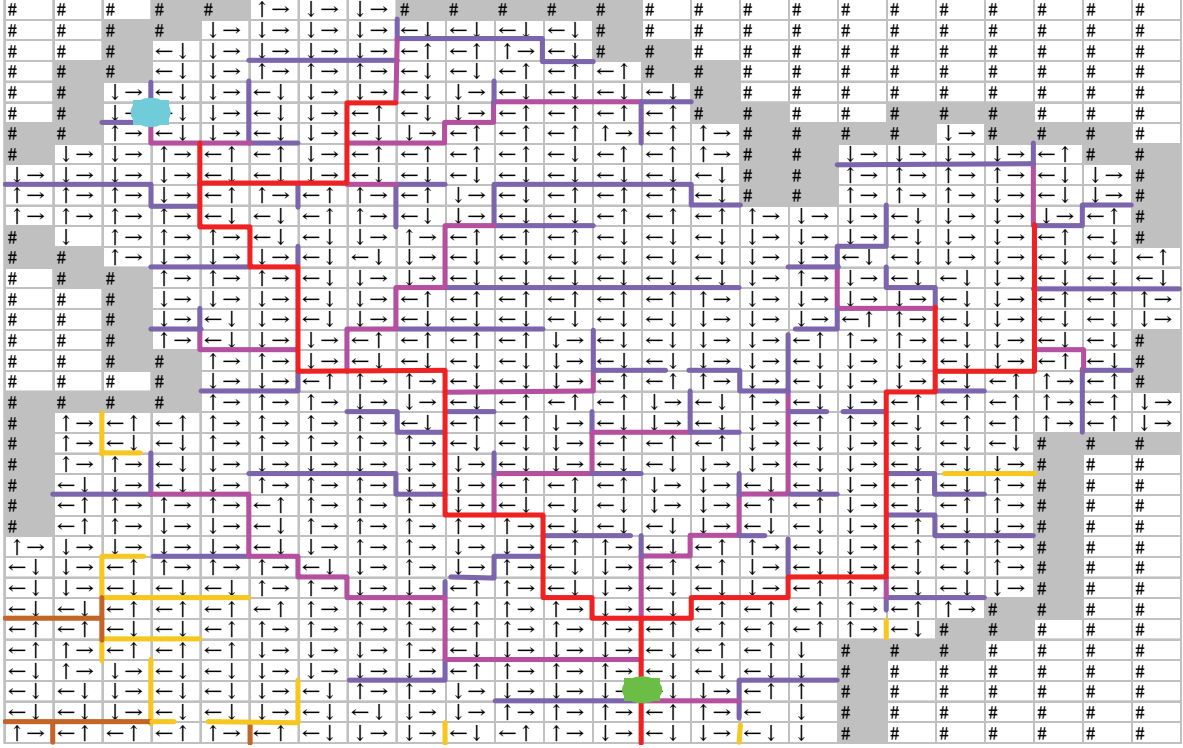


Fig. 11 Final simulated surface flow direction with 1D channel reaches and unit vectors of 2D overland flow in the x and y directions.

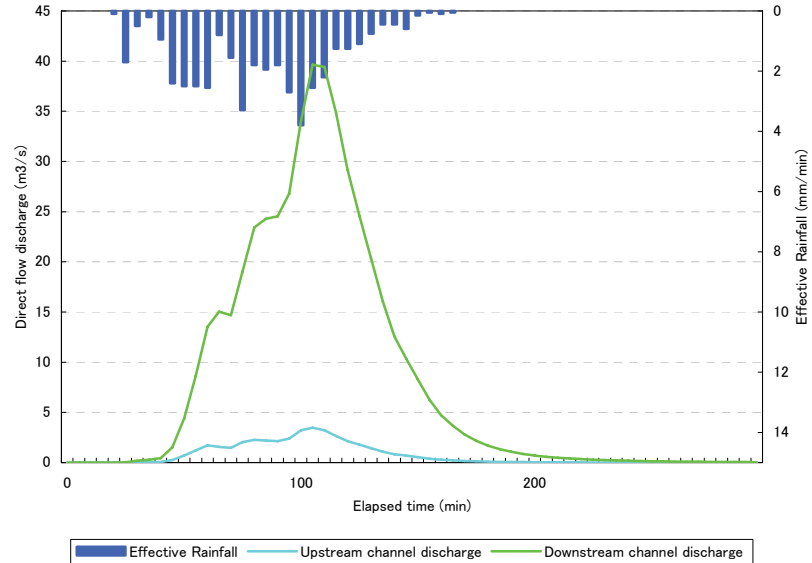


Fig. 12 Simulation results for discharge at two selected reaches (the blue and the green marks in Fig. 11)

## 6. Conclusion and further steps

To sum up briefly, the DEM-based surface flow direction can be established through four steps of simulation and corresponding manual controls (Fig. 10). In each step, the overland flow direction on each bi-linear element has been estimated by iso-parametric approximation. Then, once the

explicit channel reaches have been defined between the converging slopes, the implicit connector reaches will be established through iterative searching procedure up to twice unit distance. Thus the final topography model and the overland flow routing parameters are estimated at the end of the third step. An additional step (forth step) has been also considered to accept final manual control and

produce channel routing parameters, as well as the boundary condition at each calculation cells.

The resulting surface flow network has been depicted in Figure 10, where the unit vectors show the overland flow components in the x and y directions. As it can be seen except few adjusted channel reaches; the river network can be approximated automatically well by the converging slopes. One can come across with some DEM-based software that can also generate flow net work automatically. Nevertheless, as far as the authors are award, they can not correct the error due to uplifting DEM sinks, as our algorithm does here (Fig.9). Obviously, without such correction the slope and runoff can be underestimated.

To verify capability of the algorithm for handling flow routing application, a 2<sup>nd</sup> order Runge-Kuta FVM diffusion wave flow routing was developed to simulate surface direct flow (Hortonian) through the network. This assumption (*i.e.* no subsurface runoff) cannot be true for forested mountainous basins such as the Nagara River. However, it enables us to judge pure effect of the proposed flow configuration. Under such assumption, application of the numerical flow routing should result in different runoff picks happen at the same time. That is what can be seen in Fig.12, where by joining flow components downstream, the discharge picks tend

to unify into a larger one, but in the same time. This is just a basic verification though, and the efficiency of the proposed algorithm (such as Eq. 12) needs to be examined against observation. This requires contributing the subsurface flow components (Fig. 3) into the overland flow discharge as a follow-up of this report.

## References

- Liu, Q.Q., Chen, L. and Singh, V.P. (2004): Two-dimentional kinematic wave model of overland-flow, *J. Hydrol.*, Vol.291, pp. 28-41.
- Nasouhi, S., Hamaguchi, T., Kojiri, T. (2006): Conjunctive simulation of surface and subsurface flow within water budget, *Annals of Disas. Prev. Res. Inst., Kyoto Univ.*, No. 49 B, pp. 641-659.
- Jain, M.K., Singh, V.P. (2005): DEM-based modeling of surface runoff using diffusion wave equation, *J. Hydrol.*, Vol.302, pp. 107-126.
- Tayfur, G. (2001): Modeling two-dimensional erosion process over infiltration surfaces, *J. Hydrol. Eng.*, Vol. 6, pp. 259-262.
- Tayfur, G., Kavvas, M.L. (1994): Spatially averaged conservation equations for interacting rill-interrill area overland flows, *J. Hydraul. Eng.*, Vol. 120, pp. 1426-1448.

## 地域規模の表流水・地下水有機的利用管理のための計算システムの設定

Sina NASOUHI\*・浜口俊雄・小尻利治

\*京都大学大学院工学研究科

### 要 旨

従来の表流水・地下水有機的利用モデルの利用は平野部に限られてきたばかりか、制約のある地下水涵養シナリオでも行われてきた。そこで本研究は上記制約を打破するモデル化構成の提案を試みた。筆者らはこれまでに、基本操作ルール作成に使う解析解を算出した後、長良川支流域を用いて数値地図モデル型河道設定アルゴリズムを開発することで平野部だけでなく山岳部も加えたモデル化領域へ拡張した。本研究はGISソフトウェアで従来見かけないアルゴリズムによって、Kinematic wave法で算定された流量成分だけでなく、誤差として近似的に無視される流量成分も平野部で考慮し、様々な地形上の落水網設定に実用できることを示した。

キーワード:有機的利用、落水方向、アイソパラメトリック近似